infrastructures

MDPI

Article

Force Performance Analysis of Pile behaviour of the Lateral Load

Touré Youssouf [1]*, Tianlaiyu[1]*, Dembélé Abdramane[2], Assogba O. Cyriaque[3,] and Diakité Youssouf[3,]

[1] College of Civil Engineering, Department of civil engineering, Northeast Forestry University, No.26 Hexing Road Xiangfang District 150040., Harbin, People's Republic of China; e-mail@e-mail.com: youssoufa12@yahoo.fr; tianlaiyu@126.com

[2] Department of Automation Harbin Engineering University Heilongjiang Province, Harbin 150001, China dabdramane86@yahoo.com

[3] School of transportation science and engineering, Harbin Institute of technology, Harbin 150090, People's Republic of China e-mail@e-mail.com assocyr@stu.hit.edu.cn; youssoufdiakite07@gmail.com

* Correspondance : **Tianlaiyu[1]** e-mail@e-mail.com ; tianlaiyu@126.com Tel. : (+86-136-0451-6050)

Received: date; Accepted: date; Published: date

Abstract: The foundations allow the loads of the superstructure to be transmitted to the ground, thus the piles are generally used as a carrier transmitting loads on the ground. One of the important factors in the durability of the bridge depends more on the strength of these piles. This makes it necessary to study the reinforced concrete foundations because of their ability to resist the loads of the structure and the vertical and lateral loads applied to the structure. This implies an evaluation of the responses of the RCP (Reinforcement concrete pile) according to the different lateral loads. This study was focuses on the performance of the pile force at the lateral load of the arched bridge. The effect of the compression of the arch bridges creates a large horizontal load therefore it is one of the important factors in the dimensioning of the piles. Thus, various processing procedures were carried out by the Abaqus software, namely "soil FE modeling (Finite Element), pile FE modeling, soil-pile interface, and Mesh and boundary condition" in order to carry out an effective and predictive piles analysis. Based on the Mohr-Coulomb criterion, the soil is considered to be stratified with elastoplastic behavior, whereas the RCP were assumed to be linear isotropic elastic. Since the bridge is an arched bridge, the lateral load was applied to the head of the piles to check the pile strength, for which the displacement, stress and strain were taken into account, throughout along the pile depth. The lateral displacement of the pile shows a deformation of the soil as a function of depth, with different layers crossed with different lateral loads applied. Thus, from the study comparing the results of the FE measurements with the data measured in the field, add to the statistical analyses below, the bridge is considered to resist up to 80% for a duration of 100 years.

Keywords: Lateral Load; 3D Finite Elements; Stress; Strain; Reinforcement Concrete Pile

1. Introduction

The lateral load on the pile was performed on Yanchuan bridge in Jilin province Yanji city, in burghardtong River, China. It extends over a complete length of 324. 86 meters across the South burghardtong river. the design of the arch was chosen from an architectural purpose of view, so the bridge can be integrated into the natural site in order to extend the characteristics of the landscape of the bridge, decongest the speedily developing areas around the river additionally central city, and also to assist increase traffic. the site is regular to be around the river at the placement of the bridge, therefore it will not only be a significant part of the infrastructure for this event, it will also have to act as exhibit area for Chinese engineering. the planning of foundations on simple supports is classical (drilled piles), however the design of arch foundations is quite complex due to the low stiffness and

solidity of the soil characteristics, which this study is based on force performance analysis of reinforced concrete pile response subject to lateral load. For the Arch bridge the lateral load test is unavoidable because of the temperatures the changing in years.

Reinforced concrete piles or drilled shafts are a kind of bridge substructure during which piles or columns are continuously extended below the extent to the superstructure. This, alongside with the depth of the soil modulus and the limiting values of pile-soil contact pressure, needs to be prespecified. For the numerical methods, the analysis is done by using finite elements or finite variations. These methods will presently tackle the complete three-dimensional (3D) drawback, considering of the precise geometry, soil-structure interaction and pile effects, though such ways are in theory the most rigorous [1]– [3].

Reinforced concrete could be a standard material created by combining cement and farms with the aim of compensating for the relatively low durability and stability of RCP. Reinforcements that are mostly steel bars represent all the interconnected bars in the concrete that reinforce concrete development. Both materials have a complete consolidation because there is almost no slippage between the two and that the concrete acts in a way as a protective layer for the steel bar against corrosion.

Despite the high cost of the reinforcing steel, it reminds the recommended one for construction. It is, therefore, necessary to review the likelihood of reducing this material to the minimum throughout pile construction. In the past, piles were unquestionably strengthened [4]. Nowadays, the designers are minimizing the length of reinforcing bars; therefore, they are scaling back the value of piles [5], [6], [8] – [11], [12] – [17], [17] – [20], [21]. This reduction needs excellent separation for the cases wherever the piles would like entirely or partly reinforcement and in case, cases where the reinforcement are eliminated. From the creation survey on the codes and their field findings recommendations, codes are required to provide specifications and limitations for the share of bars that ought to be provided within the pile cross-sectional area [8], [10], [22]– [26]. However, the depth of extension of this reinforcement on the pile is not sufficient and left to the designer discretion. The main objectives of this study are: (a) building a survey of the codes and their requirements on pile reinforcement, and (b) determining the ground response using the pile to give the reinforcement, and to see the reaction of the stress and strain along the pile and the different diameter.

2. Basic Theory of Reinforcement Concrete Pile on a Lateral Load

Several researchers have developed the speculation on (p-y) curves for sand to explain the connection between soil resistance and the lateral displacement of the pile below lateral load [27], [28]. The bending of the pile is described in equation 1-6 for beam bending, and it can be seen in Figure 1.

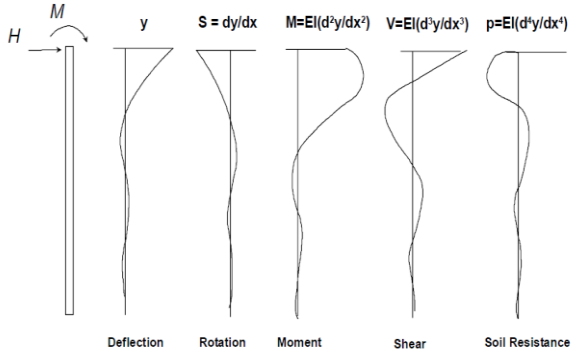


Figure 1. The deflection, rotation, moment, shear force and soil resistance of the pile foundation around the pile

$$E_P I_P \frac{d^4y}{dz^4} + Q_A \frac{d^2y}{dz^2} + E_s y = 0 \quad (1)$$

$$E_s = -\frac{p}{y} \quad (2)$$

$$S = \frac{dy}{dz} \quad (3)$$

$$M = EI\frac{d^2y}{dz^2} \quad (4)$$

$$V = EI\frac{d^3y}{dz^3} \quad (5)$$

$$p = EI\frac{d^4y}{dz^4} \quad (6)$$

Where,
y =deflection of the pile
S= slope of the deflected pile
M= moment of the pile
V= Shear
p= Soil reaction
Ep = elasticity modulus
Ip = moment of inertia of the pile
QA =load
z =depth below the pile top

The (p–y) curves are realized using the Winkler approach with uncoupled springs along the pile, where each is supporting a pile distribution. For each spring, a non-linear (p–y) curve is made. The curves were adopted and utilized in current strategies for designing lateral loaded piles within the standard codes [27], [29]. The ways are incredibly empirical as area unit they are fitted by solely a few all-out experiments represented by [8], [9], [12], [27], [30], [31]. The procedure for making the (p–y) curves for the cyclic lateral load on monopiles in the sand by [27]. The below Figure 2 shows the detail about the soil behavior and its p-y curves.

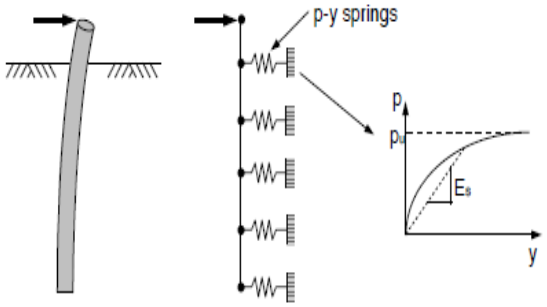


Figure 1. The principle for describing soil behavior with p-y curves

One of the main approaches for calculating the ultimate displacement because of soil yielding is the beam-on-foundation approach, where the soil is treated as plastic, and its lateral capacity is often determined from its resistance [6], [9] [15]. This method does not predict pile response since the soil resistance of the analysis is developed by empirical observation and is fitted to the numerical analysis results to satisfy the results. Another disadvantage of the (p-y) curve is that a curve developed for a particular site is not appropriate for one more site. In different countries, every site desires its (p-y)

curve is relying on the properties of the soil there, yet as a load, pile checks to predict lateral pile response accurately. This technique is therefore costly because each site requires a pile load test [9], [12]. An Associate in Narcoanalytical resolution supported an energy-based technique leading a collection of governing equations and boundary conditions. The collection of governing equations and boundary conditions, which represent the deformation of pile and soil below static lateral load has been utilized by [9], [12], [36] in homogeneous soil linear elastic and [9], [12], [37] in multi-layered nonlinear and linear elastic soil. These equations were resolved numerically employing a finite distinction technique, whereas, used an equivalent technique to predict the deformation of a pile in homogeneous linear elastic soil below dynamic lateral loads [9], [12]. In order to predict pile displacement because of lateral load, three (03) approaches are often used: the cantilever technique, Winkler's technique, and the elastic continuum technique. The cantilever method was developed by [9], [12]. In this methodology, the soil reaction is neglected, and the easy cantilever theory is employed to calculate the deformation. The distinction in the behavior of flexible and rigid piles has a much essential influence on soil behavior and the development of a "toe-kick" is essential for rigid piles.

3. Finite Element Modeling (FEM)

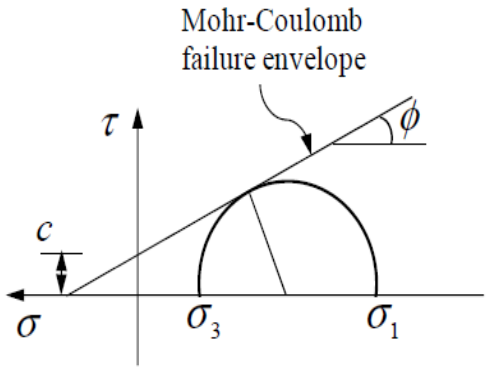
Loading on Abaqus 2017 software can be noted. The all-static loads were applied as concentrated force loads on the pile head. The symmetric geometry of the pile and the lateral deflection of the pile head was assessed under lateral loading when one was applied on the pile head. According to the solid mechanics formulations, the amount of lateral deflection can be found from Beam Flexure Theory. The pile that is placed in the soil continued up to the bedrock or hard layer. Therefore, it is often thought of as a cantilever beam [36], [38] – [41].

3.1 Soil FE Modeling

The upper, secondary, tertiary and quaternary formations of the soil consist of layers of resistant heavy weathered sandstone at different thicknesses as follows: Top 6.5 m, second 3.1m, tertiary 3.2 m, and quaternary 0.8 m. The fifth layer is intense to very dense metamorphic siltstone mudstone (8.4m). The physical and mechanical properties of the soil are indicated in Table 1. These values are given by the geotechnical investigation report (Institute of Geological Investigation of the Province of Jilin in China). It is important to say that the soil stratification adopted is comparable to that of the soil in Jilin Province (North-East China) where the "Yan song bridge@" was constructed. Recently, the behavior of the finite elements is made to describe the behavior of the geo-materials. Most complexes in a different loading handled the difficulties in the digital application and the identification parameters of the element using standard materials test procedure [22]. Elastoplastic model with models the Mohr-Coulomb failure (Mohr-Coulomb model) is usually used in finite element analysis of the Geotechnical Engineering. For reason of its simplicity and its complete accuracy in case of rupture, which is dependent on the major and minor constraints of principle ($\sigma 1$, $\sigma 3$) as shown in Figure 3. The Mohr-Coulomb model is described by the cohesion c and internal friction angle $\emptyset$ [33], [42].

$$\frac{1}{2}(\sigma_1\text{-}\sigma_3) + \frac{1}{2}(\sigma_1 + \sigma_3)\sin\emptyset\text{-}\cos\emptyset = 0 \quad (7)$$

When the distribution in the space of three-dimensional stress, the case of rupture is formed in an irregular hexagonal pyramid.



144 **Figure 2.**Mohr-Coulomb failure criterion

145 The Mohr-Coulomb model is used in geotechnical engineering practice. In this simulation, the
146 Moher Coulomb model has adopted nonlinear study behavior of the soil. In Abaqus 2017, three (03)
147 parameters are required to define the behavior of the soil. These parameters are the Density γ ',
148 friction angle Φ and Cohesion C. The elastic-modulus was taken according to the different soil
149 properties with depth. The soil was divided into five (05) layers with constant properties for every
150 layer as present in Table 1.

151 **Table 1.** Geotechnical properties of the soil

Soil			**Elasticity**		**Mohr-Coulomb**		
Quality	Layer thickness		Young's modulus (Pa)	Poisson Ratio	Density (kg/m3)	Friction angle (°)	Cohesion (Pa)
Heavy weathered sandstone	top	6.5	76,80×106	0.25	1650	25.32	34000
	Second	3.1	56.50×106	0.25	1850	28.30	2570
	third	3.2	96.70×106	0.25	1690	23.18	2200
	fourth	0.8	57.80×106	0.25	1675	26.77	2800
Metamorphic siltstone mudstone	fifth	8.4	64.20 ×106	0.25	1600	22.24	4600

152 Institute of Geological Investigation of the Province of Jilin in China

153 *3.2 Single Pile FE Modeling*

154 An ordinary reinforced concrete pile is the standard concrete pile wherever bending and Axis
155 resistance is provided by longitudinal steel bars and concrete, while transverse steel in the form of
156 hoops or spirals is used to provide concrete containment and shear strength, the concrete outside the
157 transverse steel (concrete cover) is not confined and tends to overflow as inelastic demand will
158 increase. once a bent deck pile is subjected to a lateral load, plastic hinges might form at the top of
159 the pile and below the ground. once pile is used to form pile bridge dents, each of those possible
160 hinge positions can have completely different properties and behavior. in the case of the upper hinges
161 and since of the area between the steel tube, the tube only provides containment and shear strength,
162 whereas flexural strength is mainly provided by the longitudinal bars. Conversely, for in-grounds
163 hinges, the steel tube will provide not only shear resistance and containment of the concrete, but also
164 bending resistance. As a result, the moment capacity and stiffness of the belowground hinges in the
165 pile will be considerably larger than those expected in the upper hinges. The reinforcement is FE 400

steel and was supplied by the Changchun manufacturing company in Jilin province, China, and the concrete has a compressive strength of 25 MPa.

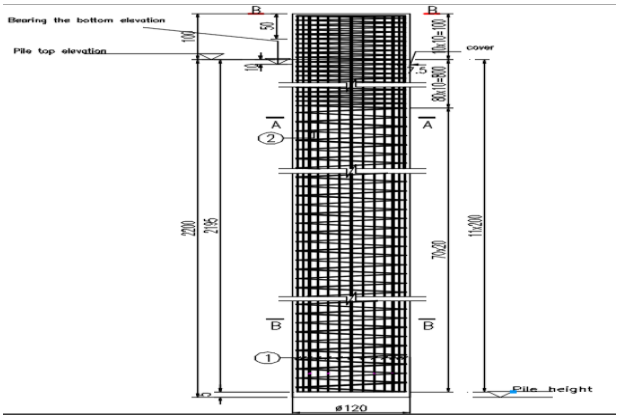
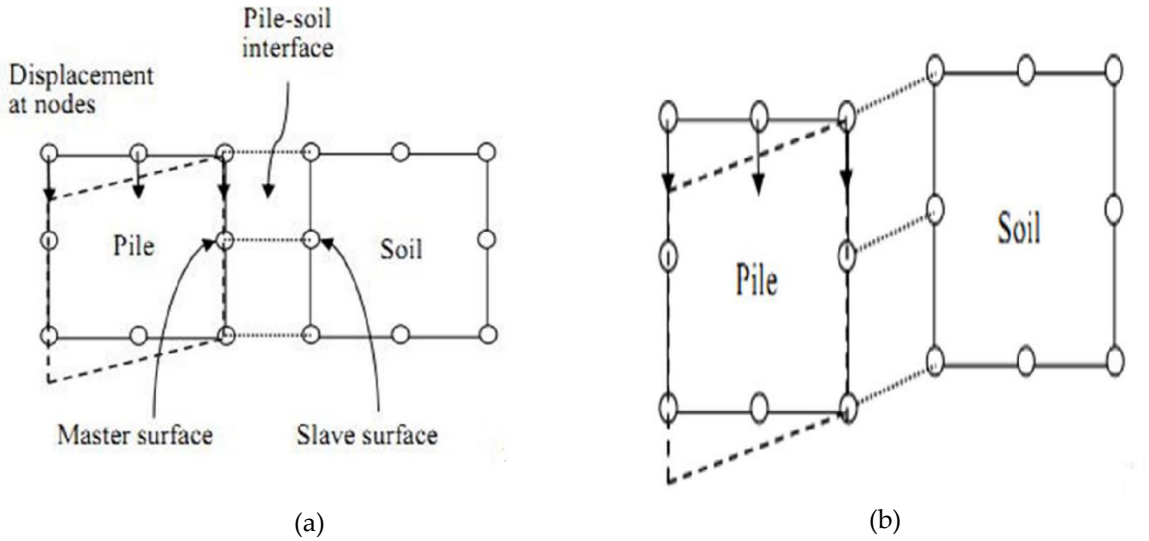


Figure 4. Modeling of the steel used for analysis the pile, Cover and reinforcement of the pile in which the concrete would be poured.

3.3 Soil-Pile Interface

The surface contact behavior of the pile-soil tangentially embraces the load transfer mechanisms in each direction. The conventional force is transferred only if the pile and soil square measure contact tightly, otherwise, it becomes zero. This type of traditional contact behavior will be present by (hard) contact choice provided by ABAQUS. The tangent behavior will vary from rough contact with no relative slippery between soil flank, and pile happens to slippery resistance conditions with no friction develops on the shaft of the pile. For contact between these two typical cases, pile resistance model in-built ABAQUS will be chosen to depict the interaction at the pile-soil interface with a prescribed resistance constant μ. These two ideal contact conditions may also be completed through the following cases: with resistance and without resistance. The soil-pile interface modeling is much essential due to its influence on the pile response below lateral loading within the soil-pile interaction, the surrounding soil and the pile elements are assumed deformable [31], [36], [39], [47]. The surface of pile elements and soil elements have a contact that the surface of pile components is selected as "Master surface," and therefore the surfaces of soil elements are defined as "Slave surface." In ABAQUS, these surfaces are known as the contact pair, and they are depicted in Figure 5. Following the suggestions created by API (1991) and Gireesha (2011) [36]. The coefficient of friction between concrete and sand relating shear stress to the normal stress was assumed to be 0.75 throughout the analysis. The "penalty function method" was utilized to represent the contact with normal contact stiffness (Kn). Once the tangent shear stress in pile-soil interface surpasses the shear resistance, relative slip between pile and soil happens. The interaction parameters used are shown in Table 2.



(a) (b)

Figure 5. Soil-pile interface modelling in Abaqus (a) No sliding, (b)Sliding

Table 2. Interaction parameters

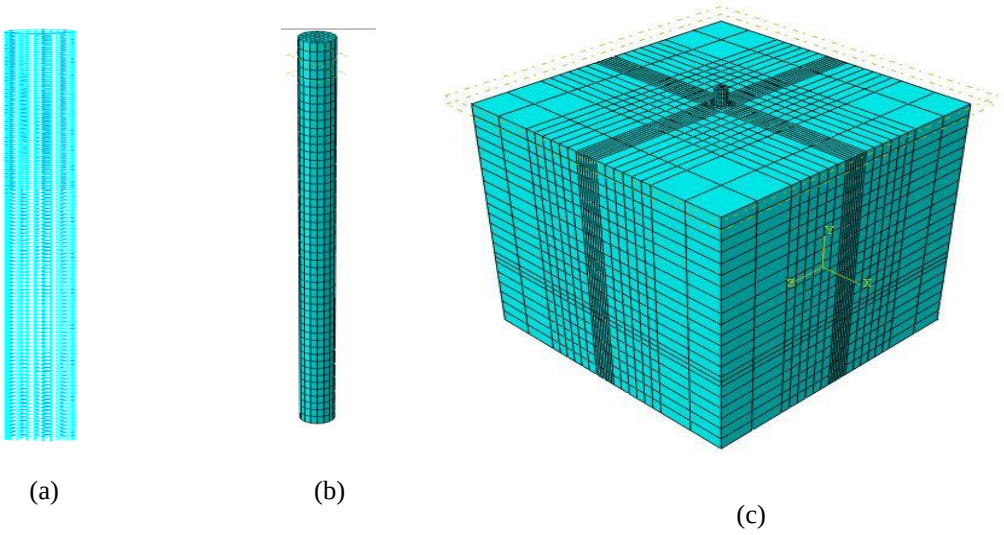
	Properties chosen for Model	**Alternative option**
Interaction	Mechanical contact<surface to surface >	<Node to surface>
Theory model	Frictional behavior contacts by Mohr-coulomb theory	Various
Sliding formulation	Small sliding	Finite sliding
Interaction properties		
Tangential behavior		
Friction formation	Penalty friction	Various
Friction coefficient [-]	0.75	0.5
Shear stress limit	No	Option limit can be set
Elastic slip, Absolute distance[m]	0.001	0.0005
Normal behavior, hard contact with penalty constraint method		
Separation after contact	Allowed	Not allowed
Tie contact for the tip of the pile	Assigned	

3.4 Mesh and Boundary Condition

The soil Mesh model was modelling using 8-node linear brick components with eight integration points (C3D8). In Figure 6c close, the pile ground is fine, and the soil far to the pile will become more and bigger. The soil material model developed within the previous section is used in modelling the confined soil. The entire geometry of the soil pile generated. The crushed stone backfill was sculpturesque mistreatment linear elastoplastic, Mohr-Coulomb failure criteria with non-associated flow rule.

The pile concrete domain was discretised utilized An 8-node linear brick, reduced integration, hourglass control (C3D8R) elements Figure 6b. Full interlocking between the sedimentary rock and therefore the soil pile is assumed. In addition, the soil pile sedimentary rock interaction was

simulated utilized two secured master/slave contact surfaces. The A2-Node linear 3-D Truss (T3D2) was used for meshing the steel bar on the pile Figure 6a,



(a) (b) (c)

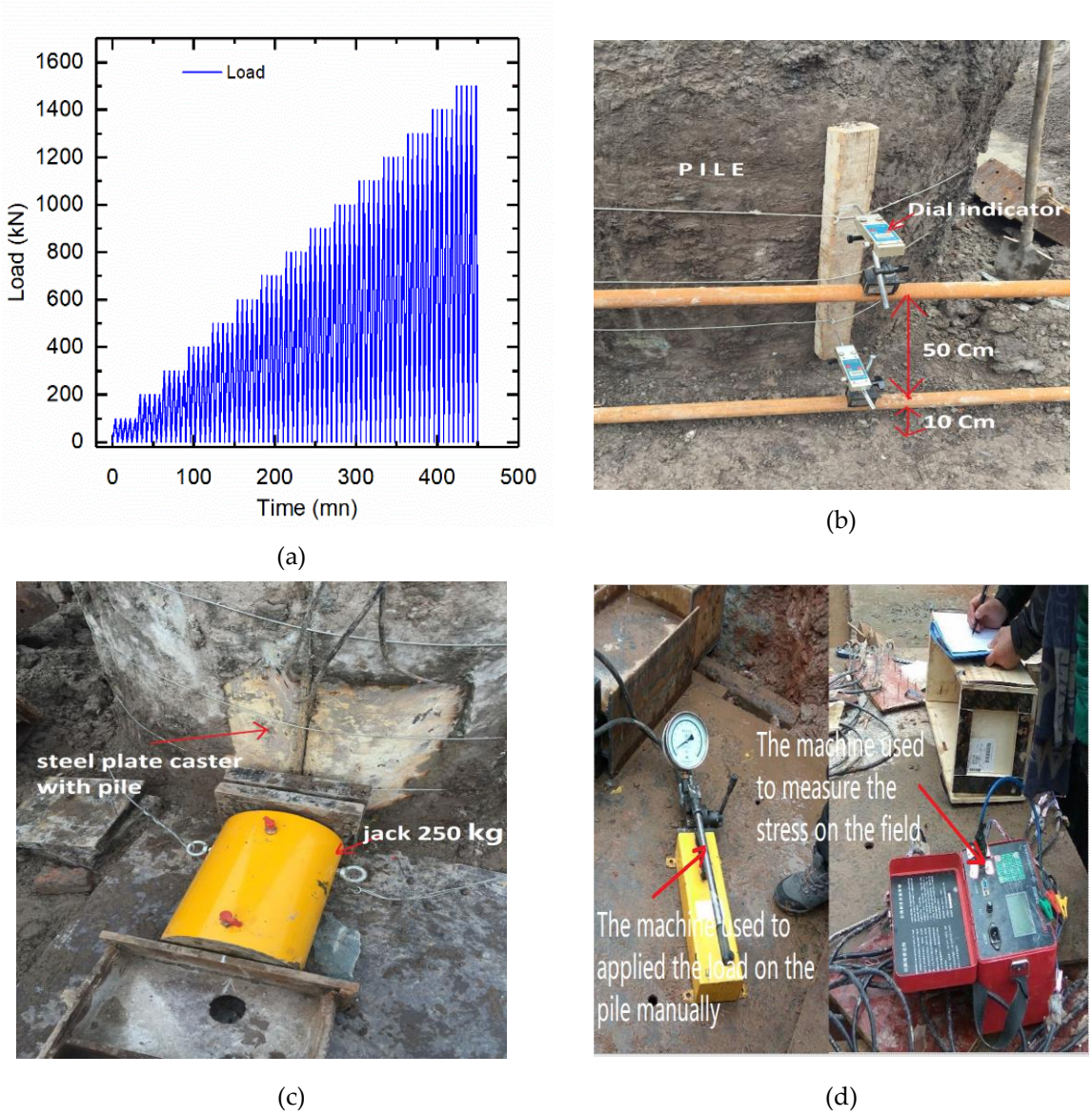
Figure 6. The meshing modeling of the soil pile(a) Steel bar; (b) RCP; (c) assembly with meshing

The pile is wholly embedded within the soil, and it is assumed to be concerning the bedrock. Therefore, the entire bearing nodes are taken as fastened assuming that the soil and pile are entirely warranted. The facet boundaries are constrained against horizontal direction, and the bottom boundaries are constrained against each horizontal and vertical directions. In addition, quiet boundaries are used for wave propagation and to eliminate "box effect" (i.e., the reflection of waves back to the model at the boundaries). In order to use the quiet boundaries to the model, infinite components are used at the boundaries.

4. FE Modeling Validation by Field Lateral Loaded Pile Test

4.1 Field Lateral Loaded Pile Testing materiel

The 22m piles were embedded into the ground with a diameter of 1.2m for an overflow of 1.5m. The piles were poured on the site and hardened for 15 days. The lateral loaded pile test was carried out on a single pile. The soil was composed of several different layers whose characteristics were presented ulterior. A 250 kg jack placed between the two piles is capable of applying up to a load of 300 tons. As shown in Figure 7c, comparators have been laid down finally measuring the displacement as a function of load Figure 7b. The load was applied using a manual machine as shown in Figure 7d. The same load applied five times is each time discharged after stabilization of 4 minutes and the unloading will be in rest for 2 minutes show on Figure 7a. The same procedure is repeated until the load reaches 1650kN.



(a) (b)

(c) (d)

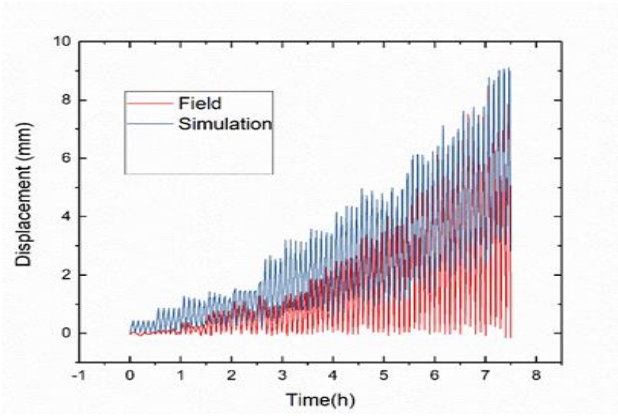
Figure 7. The material used on the field to the test ;(a) The modeling of applying a load on the pile head; (b)The pile; (c)The view of the jack;(d) The machines used to apply load and measure the stress and strain

4.2 Comparison Between FE Result and Field Measured Data

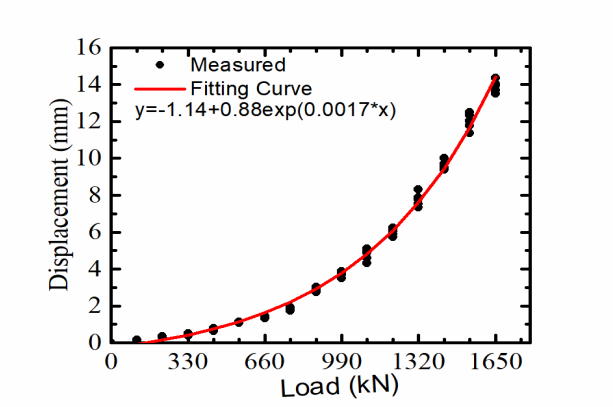
In this study, a 3-D FE modeling was developed to analyze the lateral load behavior the pile foundation driven in dense sand. The findings obtained with the analysis were compared with the experimental results determined in lateral load tests on single piles in the different soils and reinforced concrete piles. The analysis aims to validate the planned technique.

From Figure 8, the simulations show that when applying the load on the pile, the displacement on the curve of the ground is weak at the beginning of the loading (Time (h) between 0 and 1). Then after unloading, the load returns to the original place. However, as the load increases the curve of the field follows that of the simulation until it reaches. When the load is the maximum load 1650kN, the displacement on the field is 9.67 mm, and displacement from the FEM is 9.62 mm. The maximum measured displacement between the analysis from the field and FEM is 0.05mm (0.48%) at the maximum load of 1650kN. This could be explained by soil moisture and the condition of applying load on the field. Figure 8 shows the material and pile on the field. Figure 8b and c show the detail of the comparison between the field test and analysis where was taking a point on the pile. As shown in the Figure 8(b) and (c) the pile head displacement of the simulation was 14.79mm and the

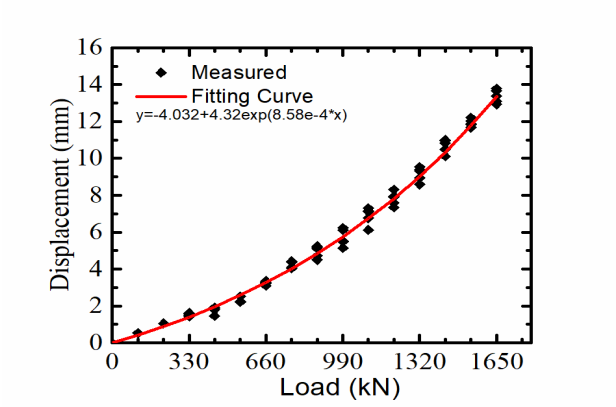
displacement of the pile head on the field was 14.74 mm either a different 0.05mm (0.48%)by applying a different lateral load (110kN to 1650kN).



(a)



(b)



(c)

Figure 8. Comparison of lateral displacement between Field measurement and FE Simulation result;(a) (H-t-Y0) the curve at the point of the test pile force FE Simulation result and field result; (b)Field measurement; (c)FE Simulation result.

5 Numerical Results and Analysis

5.1 Lateral Displacement Along the Pile

The experiments are carried out on the model of drilled piles considering the self-weight of the pile as vertical load, unlike the driven pile, which have in addition the threshing force (driving resistance of the pile). The soil deformation curves vary not only according to the nature of the layers but also the depth by applying the different loads. Therefore, there are several deformation layers and it can be noted in Figure 9 tree layers made by Abaqus. The contours of the ground deform more, once by applying lateral loads (110 kN to 1650 kN) of the pile head. The deformation according to the plain view of the soil is represented in Figure 9 while Figure 10 shows the deformation as a function of the different loads applied to the pile in the soil. The deformation is like a wave that propagates in the ground and which is the epicenter of the pile. However, this wave has strong intensity in the direction of the lateral load applied at the level of the first layers (soil 1 and 2 Figure 10a, b) and strong intensity in the opposite direction of the lateral load applied at the level of the deep layers (soil 3 Figure 10(c)). The deformations decrease with the depth of the soil.

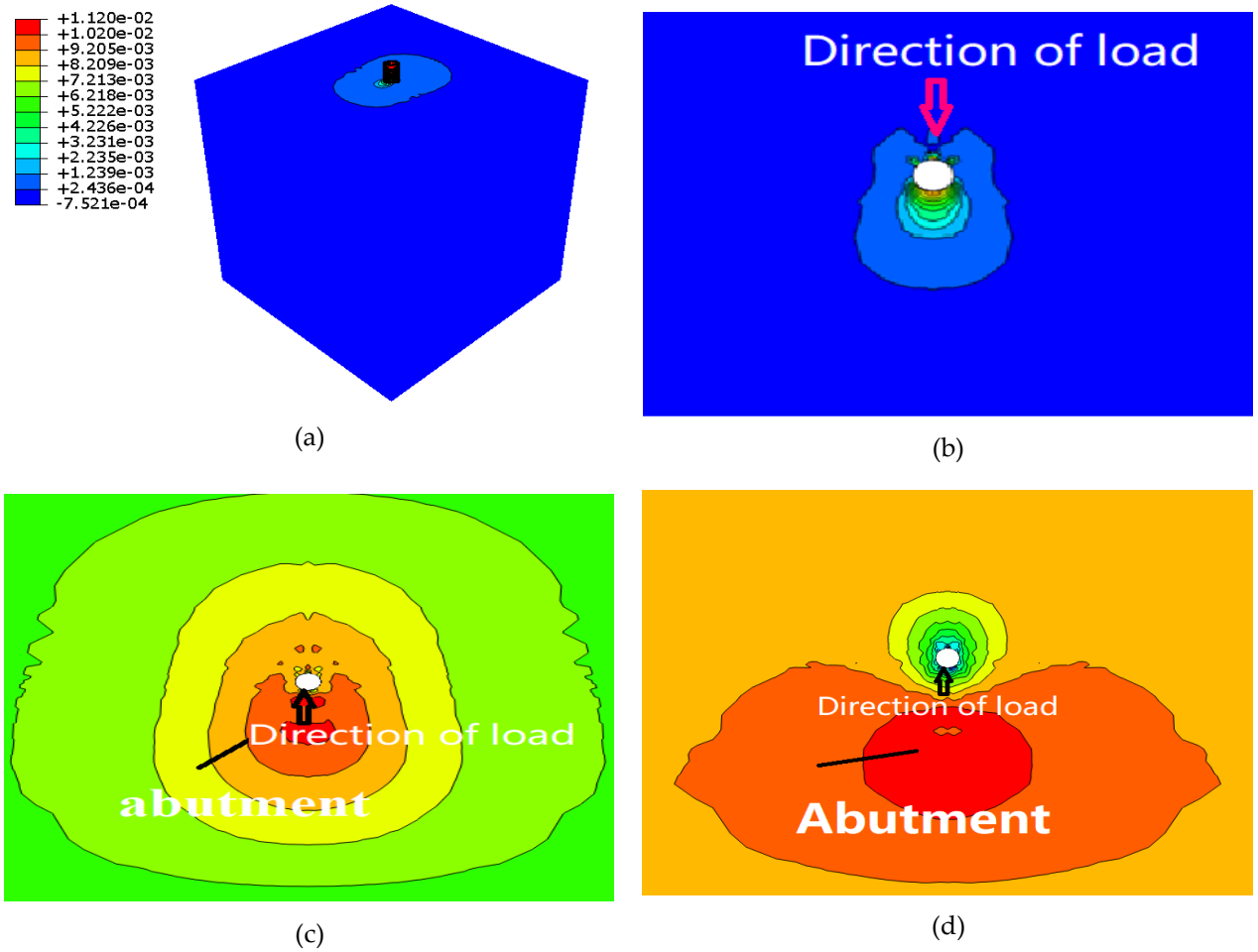
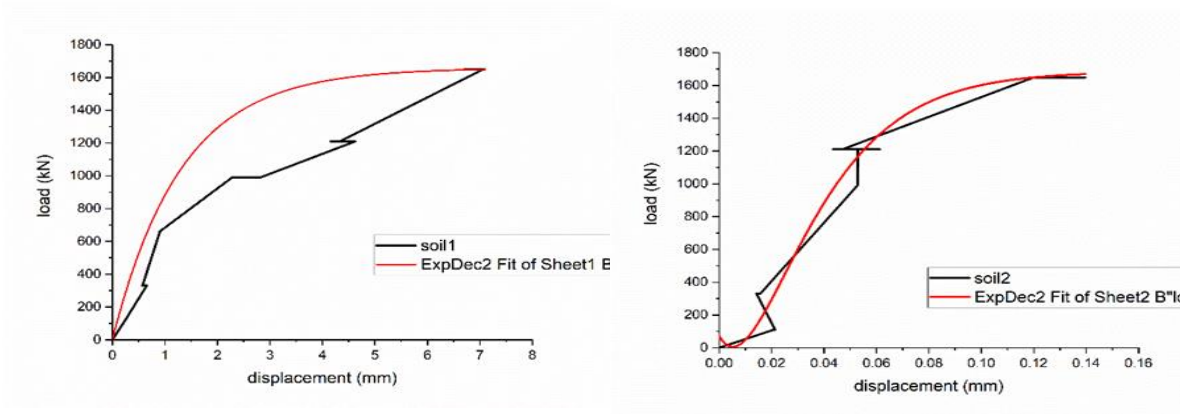
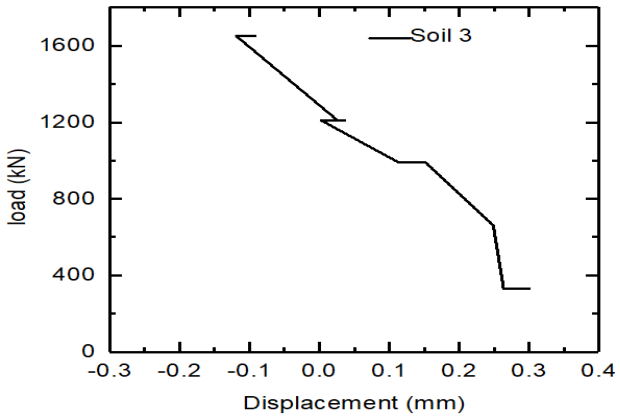


Figure 9. Plan view of Sol deformation at different depth under lateral loading; (a)Soil deformation on the lateral load; (b) Top of the first layer;(c) Top of the Second Layer; (d)Top Third Layer

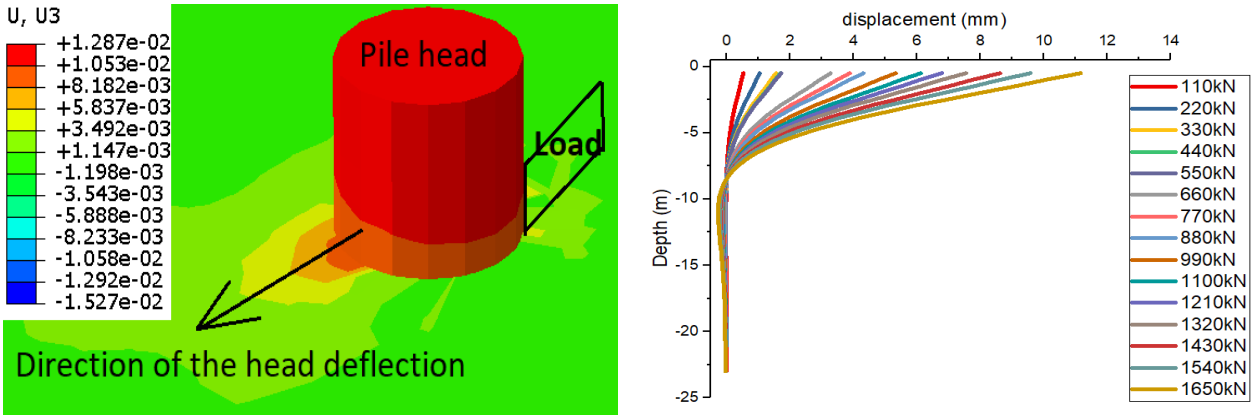




(c)

Figure 10. The relation of the first two soil displacement and the lateral load applying on the pile; (a)FE Simulation result for the soil 1; (b)FE Simulation result for the soil 2; (c)FE Simulation result for the soil 3

Figure 11 (a) Exhibits the FE deformed pile - foundation obtained at the load from 110kN to 1650kN lateral load. The distribution of piles' (Missed equivalent stress), which is shown in Figure 11(b) by the contour colors, indicating that the reinforced concrete close to the pile head at the first bend region of the pile experiences the very best stress. Figure 11(b) presents the displacement of lateral deflection generated from the FE model on pile below different lateral loads. The lateral deformation of the expected pile head at 12.87 mm is applied by the 1650kN load. The pile is inclined within the loading direction. It can be seen that the 3D FE analysis with success captures the deflection pattern of the batter pile. The deflection profiles from FEM show a slight deflection close to the pile head than the pile foot. Note, however, that the deflection curves on the pile match closely with the field measuring. It shows deformation effects at the soil surface measured near the head of the pile.



(a) (b)

Figure 3. The displacement of the lateral load on the pile head; (a) Lateral deformation of piles; (b) Lateral deformation profiles.

5.2 The Stress and strain of Steel Along the Pile

The resistance to longitudinal deformation of the pile is mainly taken up by the reinforcement, which are more resistant in traction than the concrete, which is resistant to compression, hence the usefulness of representing the stress of the reinforcement along the pile depth. And is the result of the lateral load showing the stress distribution on the pile reinforcement. The maximum stress is on 3 to 6 m depth of the pile, and the more the applied lateral load increases the maximum stress also

increases. At a depth of 12.47 m, the minimum positive stresses are found by applying the lateral load of (110 kN to 1650 kN) to the pile head as shown in Figure 12(b).

The strain curve is plotted by choosing the same points as the stress along the pile and is a function of the depth. And it observes that stress and stress are proportional, but of opposite direction from which the maximum strain has a depth of 3 to 6 m of the pile, and the minimum is 12.47 m deep. It is also noted for different lateral loading cases that there is a constant relationship between strain and stress for example, for the loading case of 1650 KN a maximum stress of about 9 MPa is obtained and a maximum strain of about -30 which gives a constant value of about 3 m. This constant can be justified by the fact that the relationship between these two parameters is the Young's modulus which remains constant for the same material and represents the slope (Hooke's law).

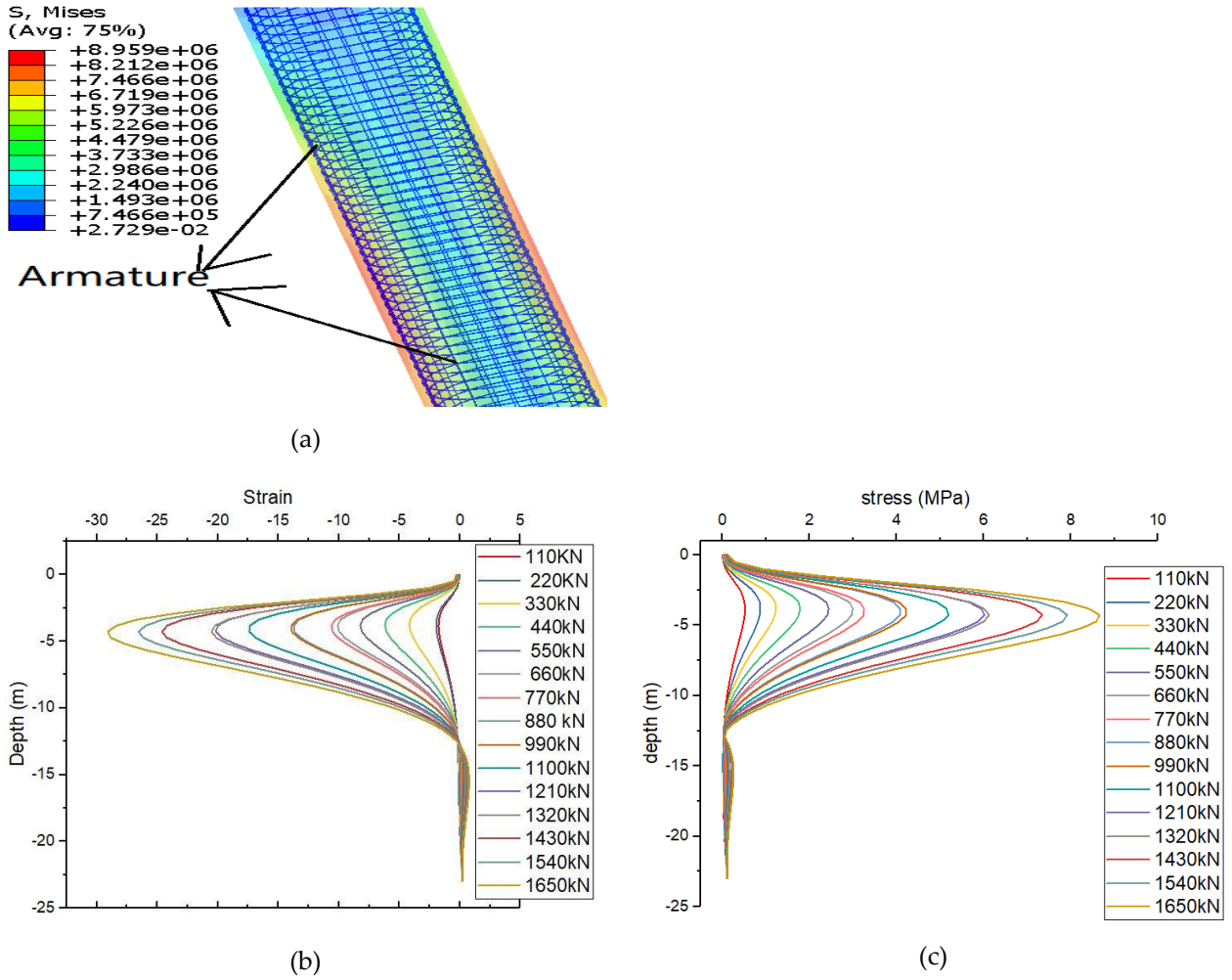
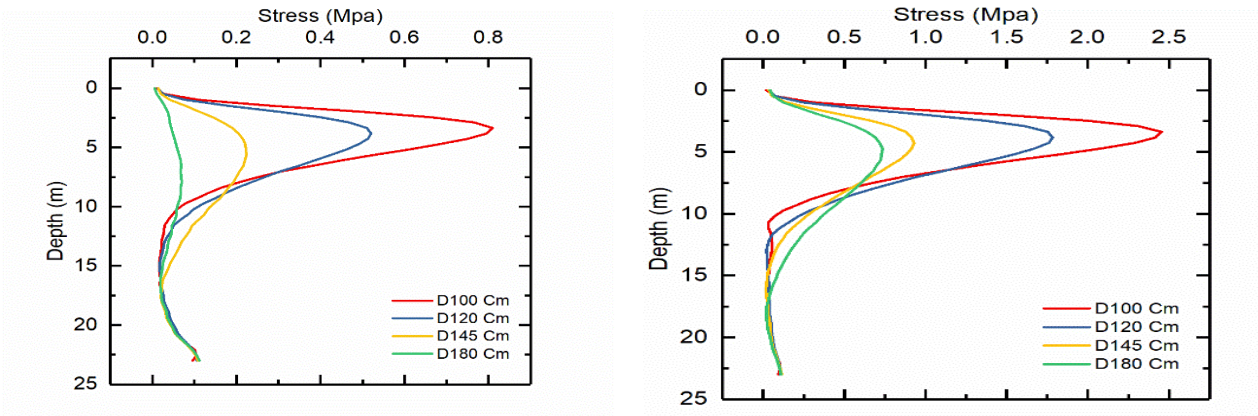


Figure 12. stress and strain of a lateral load of steel along the pile; (a) the Steel bar modeling; (b) the strain of lateral of steel along the pile; (c) the stress of lateral of steel along the pile

5.3 Effect of Reinforced Concrete Pile Diameter

Four different diameters (D = 1.00m, D = 1.2m, D = 1.45m and D = 1.8m) were chosen to study pile geometry impact at the load (110 kN, 440 kN, 1100 kN and 1650 kN). The pile is supposed to be elastoplastic, and the soil is made using the behavioral relationship of Mohr-Coulomb [1], [11], [14], [16], [28], [29]. Figure 13 shows the result of pile diameter on the stress distribution on the pile shaft. The increase of pile diameter will increase the pile stiffness and consequently can decrease the number of tensile stresses on the shaft. The most tensile stress and strain can decrease at a depth move between 4.28 to 4.73m for a pile diameter of 1.0 to 1.8 m, respectively. The depth of zero tensile stress decreases as the function of the pile diameter increasing. However, typically, it does not exceed diameters. Once the pile diameter increases, the moment of inertia of its section can increase too, that causes a reduction in stresses and strain Figure 13 and Figure 13. The lateral displacement distributions in function of different pile diameters are illustrated in Figure 14. The combination the finishes up in Figure 14 shows that the lateral displacements of the pile shaft decrease step by step in function of the pile diameter. Once applying the load of 1650 kN to the different pile diameters (1.0m to 1.8m) the differences between the displacements are perceptible. For example, the application of 1650 kN to pile diameters 1.0m and 1.2m cause a slight lateral displacement (decreasing) of the pile shaft from 29.93mm to 12.57mm. Thus, the same proportion trend is observed at the level of different loads (110 kN, 440 kN, 1100 kN, and 1650 kN) applied to the different diameters (1.0, 1.20, 1.45, and 1.80 m). Therefore, the displacement decreases when the diameter increase. The linear relationship is developed progressively at different types of soil interface Figure 14, which will be taken from 2 aspects. On the one hand, the loading of the pile shaft can increase non-linearly with the increase in pile diameter that is useful to the increase the intervals of the lateral resistance of the pile shaft. On the other hand, enlarged pile diameter expands the pile-soil contact area (linear reaction between pile-soil contact area and pile diameter). As a result of the resistance force between pile shaft and soil flank, the lateral displacement of soil flank will cause lateral stress and strain on the pile shaft and thereby a lateral displacement of the pile shaft. Therefore, the ultimate variation law of the lateral displacement of the pile body used to figure out that between the loadings or lateral friction of piles takes the dominant role. The loading takes the dominant role during this case.



(a) (b)

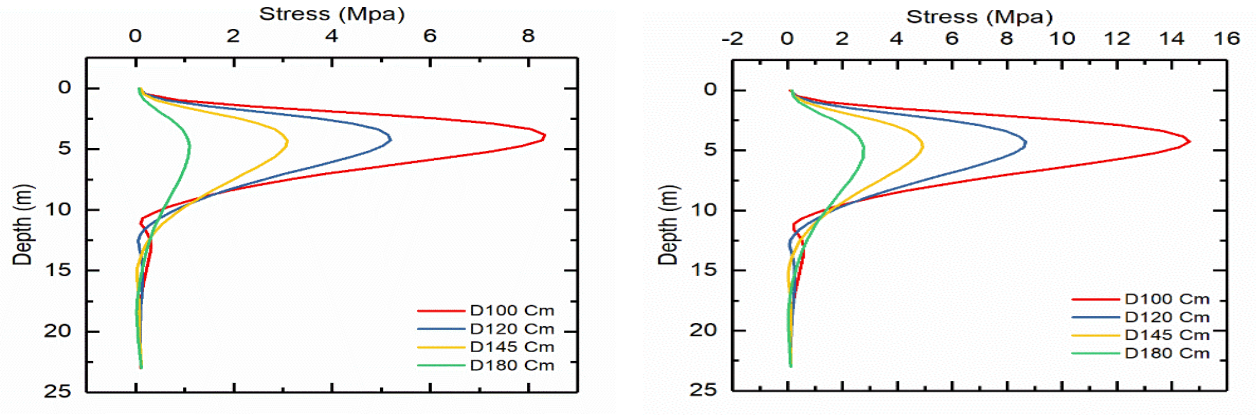


Figure 13. Impact of diameter on the stress distribution along of reinforced concrete pile; (a) The stress of the pile in the function different diameters at load 110kN; (b) The stress of the pile in the function different diameters at load 440kN; (c) The stress of the pile in the function different diameters at load 1100kN, (d) The stress of the pile in the function different diameters at load 1650kN.

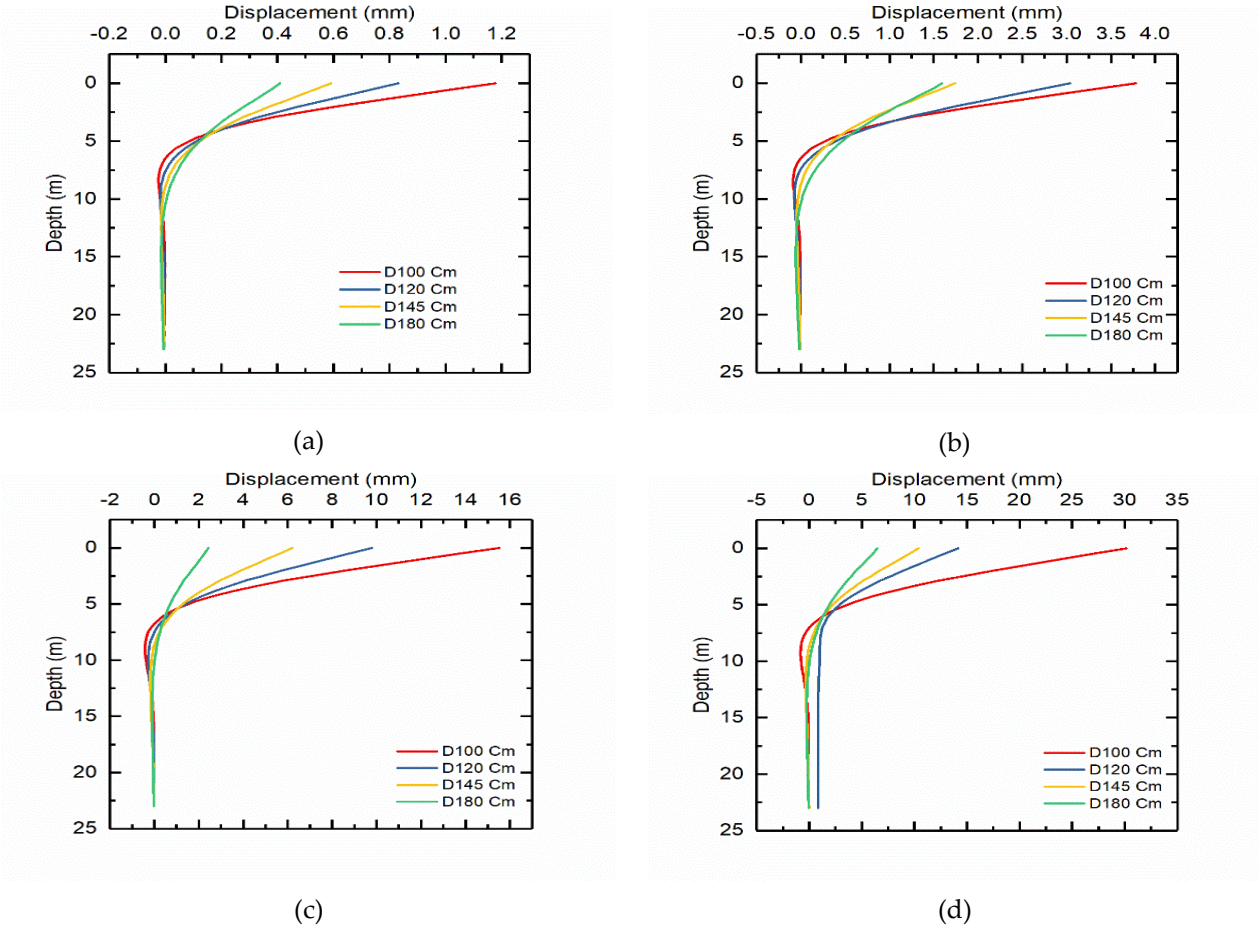


Figure 14. Impact of diameter on the displacement distribution along of reinforced concrete pile; (a) The displacement of the pile in the function different diameters at load 110kN; (b) The displacement of the pile in the function different diameters at load 440kN; (c) The displacement of the pile in the function different diameters at load 1100kN(d) The displacement of the pile in the function different diameters at load 1650kN

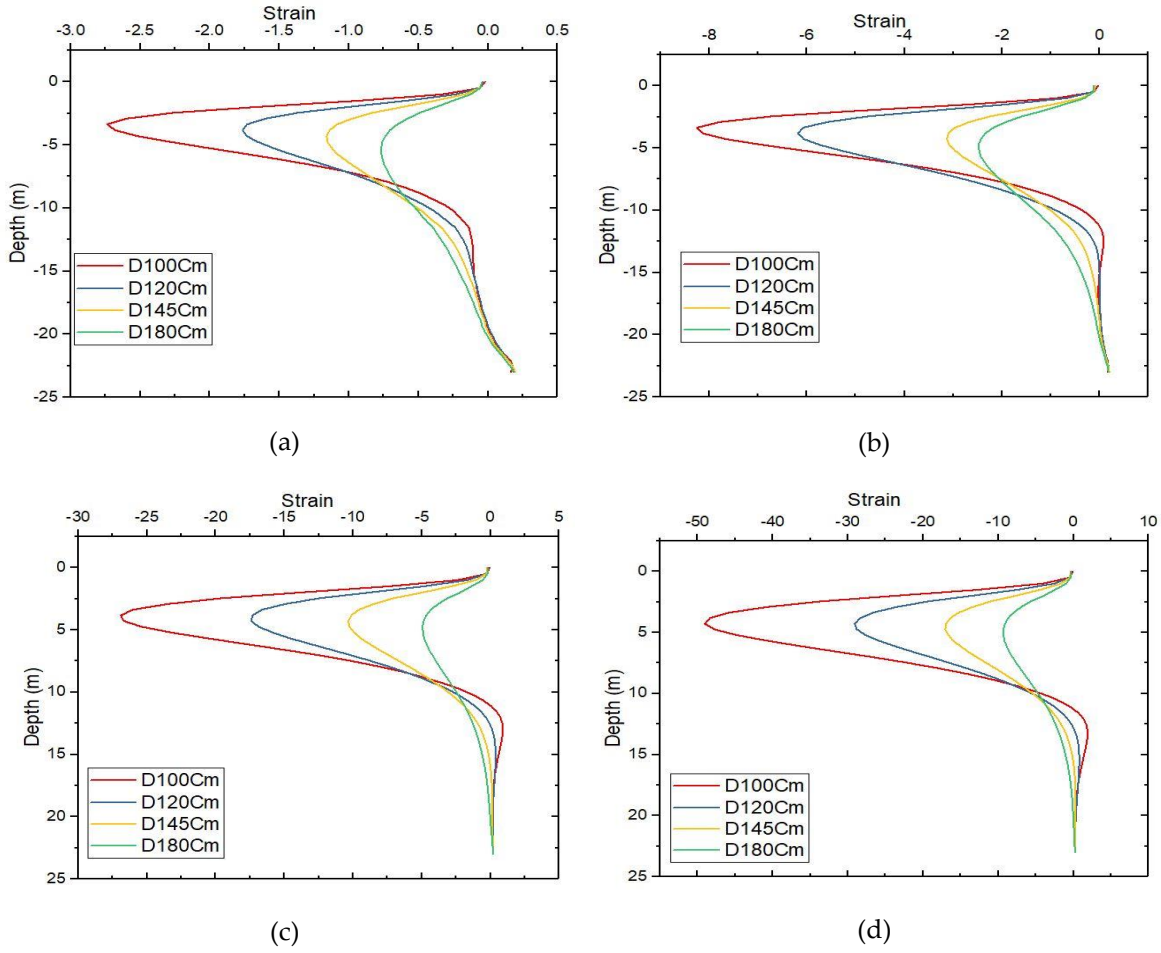


Figure 15. Impact of diameter on the strain distribution along of reinforced concrete pile, (a) The strain of the pile in the function different diameters at load 110kN, (b) The strain of the pile in the function different diameters at load 440kN, (c) The strain of the pile in the function different diameters at load 1100kN, (d) The strain of the pile in the function different diameters at load 1650kN.

After analysis of the different curves, it is noted that according to the different lateral load cases apply the stress are:

- inversely proportional to diameter (more the diameter is large, more the stress decrease)

- proportional to the horizontal displacement of the piles (more the stress increase, more the horizontal displacement of the piles increases)

- proportional and opposite direction to the strain (more the stress increases and the more the strain increases but the direction is negative) In additionally, the difference between the displacement decreases as shown in Figure 14 (d). However, the choice of diameter is made by respecting not only the permissible displacement of the piles, which is between (30 and 40mm), but also to satisfy the financial ratio and the safety factor. The soil being known to be heterogeneous with a significant safety factor will cover the solicitations due to time, hence the choice to make a comparison between the different types of diameter: D = 100 cm, d = 29,93 mm, while the displacement of the diameter D = 120 cm, 12,87 mm.

6. Conclusions

The main objective of this paper was to study the performance force of reinforced concrete pile coherent soil under lateral load. From the finite element modelling process, the static analysis of the RCP was established by calculate displacement, stress and strain response along the RCP to the different soil layer. Then, has been generated the conclusion below following the comparison between the RCP simulation carried out by the Mohr-Coulomb model used in Abaqus, and the field measurement.

1-after a comparison between the simulation and the field measurement, it can be seen that at the beginning of applied load, the displacement of the pile from the field is smaller than the simulation. When the load increases the displacement of the field and the simulation are almost follows, which when applied the final load 1650kN the displacement of the field is 9,67 mm, while that of the simulation is 9,62 mm.

2 - after the application of the various lateral loads on the pile head, it was found that the deformation of the soil varies depending on the soil layer. And it was constant that at a depth of 6m there is the displacement zeros by applying different lateral loads on the pile head (110kN to 1650kN).

3-it can be concluded that taking a point on the head of the pile the maximum displacement of the field was 14.74 mm and the displacement of the simulation was 14.79 mm, either 0.05 mm (0.48%) difference which is acceptable for validating the simulation.

4-it can be noted that taking into account the field and the simulation the maximum stress and strain on the pile body is at a depth of 5 m and point where the stress and strain returns to 0 was at a depth of 13m, it can be noted that stress and strain have opposite directions.

Funding: This research received no external funding.

Conflicts of Interest: The author declares no conflict of interest.

Acknowledgments

The author would like to thank the Northeast Forestry University Forest and his supervisor for valuable suggestion to facilitate this project. Also, extend his gratitude to the Chinese Government converted by Northeast Forestry University and particularly all members of the department of civil engineering. Additionally, we are also grateful to the reviewers and co-editor for their valuable comments and suggestions for this paper.

References

1. R. Kourkoulis, F. Gelagoti, I. Anastasopoulos, And G. Gazetas, "Slope Stabilizing Piles and Pile-Groups: Parametric Study and Design Insights," J. Geotech. Geoenvironmental Eng., Vol. 137, No. 7, Pp. 663–677, 2011.
2. R. Di Laora, R. M. S. Maiorano, And S. Aversa, "Ultimate Lateral Load Of Slope-Stabilising Piles," Geotech. Lett., Vol. 7, No. 3, 2017.
3. D. Mujah, F. Ahmad, H. Hazarika, And N. Watanabe, "The Design Method of Slope Stabilizing Piles: A Review," Int. J. Curr. Eng. Technol., Vol. 3, No. 2, Pp. 224–229, 2013.
4. A. Jain, T. Gupta, And R. K. Sharma, "Measurement and Repair Techniques of Corroded Underwater Piles: An Overview," Vol. 6, No. 7, Pp. 19–27, 2016.
5. Y. Cai, B. Tu, J. Yu, Y. Zhu, And J. Zhou, "Numerical Simulation Study on Lateral Displacement of Pile Foundation and Construction Process Under Stacking Loads," Complexity, Vol. 2018, Pp. 1–17, 2018.
6. M. Mardfekri, P. Gardoni, And J. M. Roesset, "Modeling Laterally Loaded Single Piles Accounting for Nonlinear Soil-Pile Interactions," J. Eng. (United States), Vol. 2013, 2013.
7. P. Kavitha, M. M. Venkatesh, And R. Sundaravadivelu, "Soil-Structure Interaction Analysis of a Dry Dock," Aquat. Procedia, Vol. 4, No. Icwrcoe, Pp. 287–294, 2015.

8. F. A. Salman, M. M. Mohammed, S. M. Shirazi, And M. Jameel, "Reinforcement in Concrete Piles Embedded in Sand," Int. J. Phys. Sci., Vol. 5, No. 15, Pp. 2259–2271, 2010.
9. D. E. Online, "Durham E-Theses Analytical Methods for Predicting Load-Displacement Behaviour of Piles," 2014.
10. C. Sections, "Analysis Methods for Laterally Loaded Pile Groups Using an Advanced Modeling of Reinforced Concrete Sections," 2018.
11. D.-P. Kontoni And A. Farghaly, "3d Fem Analysis of a Pile-Supported Riverine Platform Under Environmental Loads Incorporating Soil-Pile Interaction," Computation, Vol. 6, No. 1, P. 8, 2018.
12. F. Hashem-Ali, Salma, "Analytical Methods for Predicting Load-Displacement Behaviour Of Piles," 2014.
13. K. Cui, J. Feng, And C. Zhu, "A Study on The Mechanisms of Interaction Between Deep Foundation Pits and The Pile Foundations of Adjacent Skewed Arches as Well as Methods for Deformation Control," Vol. 2018, 2018.
14. K. Abdel-Rahman And M. Achmus, "Numerical Modelling of Combined Axial and Lateral Loading of Vertical Piles," Numer. Methods Geotech. Eng. - 6th Eur. Conf., Pp. 575–581, 2006.
15. B. T. Kim And G. L. Yoon, "Laboratory Modeling of Laterally Loaded Pile Groups in Sand," Ksce J. Civ. Eng., Vol. 15, No. 1, Pp. 65–75, 2011.
16. H. A. Shaia And S. A. Abbas, "Three-Dimensional Analysis Response of Pile Subjected to Oblique Loads," Vol. 6, No. 2, Pp. 508–511, 2015.
17. A. Abdel-Mohti And Y. Khodair, "Analytical Investigation of Pile-Soil Interaction in Sand Under Axial and Lateral Loads," Int. J. Adv. Struct. Eng., Vol. 6, No. 1, 2014.
18. V. S. Phanikanth, D. Choudhury, And G. Rami Reddy, "Response of Single Pile Under Lateral Loads In Cohesionless Soils," Electron. J. Geotech. Eng., Vol. 15 H, Pp. 1–18, 2010.
19. A C. I. Committee, "Aci 543r-00 Design, Manufacture, And Installation of Concrete Piles," Construction, Vol. 00, No. Reapproved, Pp. 1–49, 2005.
20. J. D. Schall And G. R. Price, National Cooperative Highway Research Program: Report 515. 2004.
21. T. Kanakeswararao And B. Ganesh, "Analysis of Pile Foundation Subjected to Lateral and Vertical Loads," No. 2, Pp. 113–127, 2017.
22. A. A. Niyaz, A. Junaid, A. Shafeeque, B. Mohd, A. Sadique, And K. A. Noor, "Pile-Soil Interaction by Finite," No. 2, Pp. 2016–2017.
23. S. Balendra, "Numerical Modeling of Dynamic Soil-Pile-Structure Interaction," Dep. Civ. Eng., Vol. Master Of, No. December 2005.
24. F. A. Salman, M. Y. Fattah, M. M. Mohammed, And R. Hashim, "Numerical Investigation on Reinforcement Requirement For Piles Embedded In Clay," Sci. Res. Essays, Vol. 5, No. 18, Pp. 2731–2741, 2010.
25. D. A. Brown, M. W. O'Neill, M. Hoit, M. Mcvay, M. H. El Naggar, And S. Chakraborty, "Static and Dynamic Lateral Loading Of Pile Groups," Natl. Coop. Highw. Res. Progr., No. Report 461, P. 50, 2001.
26. "Selection of Pile Foundation:" 2010.
27. L. Rasmussen, K. Wolf, L. Bo, And K. L. Rasmussen, "A Literature Study on The Effects Of Cyclic Lateral Loading Of Monopiles In Cohesionless Soils," 2013.
28. C. Favaretti, "Towards Next Generation P-Y Relationships: Part 1 Report Part 1 : State Of Practice – State Of The Art."
29. B. Wrana, "Pile Load Capacity – Calculation Methods," Stud. Geotech. Mech., Vol. 37, No. 4, 2015.
30. F. The report, "Pile Group Program For Full Material Modeling And Progressive Failure," Contract, No. December 2008.
31. A. Dodds And G. Martin, "Modeling Pile Behavior In Large Pile Groups Under Lateral Loading," 2007.
32. "Graduate School Of Natural And Applied Sciences An Investigation Of The Behavior Of Fiber Reinforced Concrete Piles Under An Investigation Of The Behavior Of," 2011.
33. K. Johnson, P. Lemcke, W. Karunasena, And N. Sivakugan, "Modelling The Load E Deformation Response Of Deep Foundations Under Oblique Loading," Vol. 21, Pp. 1375–1380, 2006.
34. K. Johnson, P. Lemcke, W. Karunasena, And N. Sivakugan, "Modelling The Load-Deformation Response Of Deep Foundations Under Oblique Loading," Environ. Model. Softw., Vol. 21, No. 9, Pp. 1375–1380, 2006.

35. L. Hazzar, M. N. Hussien, And M. Karray, "Influence Of Vertical Loads On Lateral Response Of Pile Foundations In Sands And Clays," J. Rock Mech. Geotech. Eng., Vol. 9, No. 2, Pp. 291–304, 2017.
36. [36] N. Rahemi, "Numerical Investigation On Lateral Deflection Of Single Pile Under Static And Dynamic Loading," 2012.
37. D. Bahloul And B. Moussai2, "Three-Dimensional Analysis Of Laterally Loaded Barrette Foundation Using Plaxis 3d," Tanda Kardinal Pemeriksaan Eksternal Jenasah Diduga Tenggelam Dari Data Bagian Ilmu Kedokt. Forensik Rsup Sanglah Bali Tahun 2012 -2014, Vol. 4, No. 5, Pp. 29–42, 2015.
38. M. H. El Naggar And K. J. Bentley, "Dynamic Analysis For Laterally Loaded Piles And Dynamic P-Y Curves," Can. Geotech. J., Vol. 37, No. 6, Pp. 1166–1183, 2000.
39. K. J. Bentley And M. H. El Naggar, "Numerical Analysis Of Kinematic Response Of Single Piles," Can. Geotech. J., Vol. 37, No. 6, Pp. 1368–1382, 2000.
40. M. Heidari, M. Jahanandish, H. El Naggar, And A. Ghahramani, "Nonlinear Cyclic Behavior Of Laterally Loaded Pile In Cohesive Soil," Can. Geotech. J., Vol. 51, No. 2, Pp. 129–143, 2014.
41. A. Rahmani, M. Taiebat, W. D. L. Finn, And C. E. Ventura, "Evaluation Of P-Y Curves Used In Practice For Seismic Analysis Of Soil-Pile Interaction," Geocongress 2012, No. May, Pp. 1780–1788, 2012.
42. Y. G. Zhan, H. Wang, And F. C. Liu, "Modeling Vertical Bearing Capacity Of Pile Foundation By Using Abaqus," Electron. J. Geotech. Eng., Vol. 17 M, Pp. 1855–1865, 2012.
43. H. Qu, "Hysteresis Analysis On Beam-Column Connection Of Concrete-Filled Steel Tubular Structure Under Cyclic Loading," Trans Tech Publ. Switzerlandineering Mater., Vol. 517, Pp. 376–381, 2012.
44. M. A. Najafgholipour, S. Dehghan, A. Dooshabi, And A. Niroomandi, "Finite Element Analysis Of Reinforced Concrete Beam-Column Connections With Governing Joint Shear Failure Mode.," Lat. Am. J. Solids Struct., Pp. 1200–1225, 2017.
45. G. Voyiadjis And Z. Taqieddin, "Elastic-Plastic And Damage Model For Concrete Materials: Part I-Theoretical Formulation," Int. J. Struct. Chang. Solids, Vol. 1, No. 1, Pp. 31–59, 2009.
46. M. Asadi, "E Xperimental Test And F Inite E Lement M Odelling Of Pedestrian," Test, No. Figure 1, P. 60876, 2010.
47. B. K. Maheshwari, K. Z. Truman, M. H. El Naggar, And P. L. Gould, "Three-Dimensional Finite Element Nonlinear Dynamic Analysis Of Pile Groups For Lateral Transient And Seismic Excitations," Can. Geotech. J., Vol. 41, No. 1, Pp. 118–133, 2004.